Reversible single cell trapping of Paramecium caudatum to correlate swimming behavior and membrane state

Lukas G. Schnitzler, Anne Paeger, Manuel S. Brugger, Matthias F. Schneider, Christoph Westerhausen

Angaben zur Veröffentlichung / Publication details:

Schnitzler, Lukas G., Anne Paeger, Manuel S. Brugger, Matthias F. Schneider, and Christoph Westerhausen. 2022. "Reversible single cell trapping of Paramecium caudatum to correlate swimming behavior and membrane state." *Biomicrofluidics* 16 (2): 024102. https://doi.org/10.1063/5.0084084.

Biomicrofluidics

Reversible single cell trapping of *Paramecium caudatum* to correlate swimming behavior and membrane state

Cite as: Biomicrofluidics **16**, 024102 (2022); https://doi.org/10.1063/5.0084084
Submitted: 03 January 2022 • Accepted: 15 February 2022 • Published Online: 03 March 2022

Lukas G. Schnitzler, Anne Paeger, Manuel S. Brugger, et al.

Biomicrofluidics ARTICLE scitation.org/journal/bmf

Reversible single cell trapping of *Paramecium caudatum* to correlate swimming behavior and membrane state

Cite as: Biomicrofluidics **16**, 024102 (2022); doi: 10.1063/5.0084084
Submitted: 3 January 2022 · Accepted: 15 February 2022 ·
Published Online: 3 March 2022

Lukas G. Schnitzler,[1,2] Anne Paeger,[3] Manuel S. Brugger,[1,2] Matthias F. Schneider,[3] and Christoph Westerhausen[2,4,5,a)]

AFFILIATIONS

[1]Institute of Physics, Experimental Physics I, University of Augsburg, 86159 Augsburg, Germany
[2]Center for NanoScience (CeNS), Ludwig-Maximilians-Universität Munich, 80799 Munich, Germany
[3]Medical and Biological Physics, Technical University Dortmund, 44227 Dortmund, Germany
[4]Augsburg Center for Innovative Technologies (ACIT), 86159 Augsburg, Germany
[5]Physiology, Institute of Theoretical Medicine, University of Augsburg, 86159 Augsburg, Germany

[a)]**Author to whom correspondence should be addressed:** christoph.westerhausen@gmail.com

ABSTRACT

Single cell measurements with living specimen like, for example, the ciliated protozoan *Paramecium caudatum* can be a challenging task. We present here a microfluidic trapping mechanism for measurements with these micro-organisms that can be used, e.g., for optical measurements to correlate cellular functions with the phase state of the lipid membrane. Here, we reversibly trap single cells in small compartments. Furthermore, we track and analyze the swimming behavior of single cells over several minutes. Before and after reversible trapping the swimming speed is comparable, suggesting that trapping does not have a large effect on cell behavior. Last, we demonstrate the feasibility of membrane order measurements on living cells using the fluorescent dye 6-lauryl-2-dimethylaminonaphthalene (Laurdan).

INTRODUCTION

During the past 300 years, paramecia have been reported from practically every part of planet Earth. The freshwater species are commonly found in pools, ponds, lakes, aquaria, reservoirs, bodies of stagnant water, streams, rivers, and, occasionally, drinking water. Due to this fact, it is not surprising that paramecia are one of the most studied micro-organisms in biology. The effects of several chemical and physical factors on paramecia have been investigated intensively. These include, among others, food, pH, temperature, ultraviolet and visible light, drugs, various chemicals, electric current, magnetic fields, sound waves, bioelectrical phenomena, and even space flights.[1]

Studies on cellular processes are often performed with large cell populations. However, parameters measured as averages of large populations can be misleading. An apparently linear response to a signal might actually reflect an increasing number of cells in the population that have switched from "off" to "on" rather than a uniform increase in the response of all cells.[2] Moreover, dynamic single-cell measurements require methods capable of holding an individual cell in place for repeated measurements, and it is important that the cell behavior is not perturbed by cell handling methods.[3]

Observing the behavior and tracking of individual paramecia cells is still a challenge due to their high mobility. Under optimal conditions, paramecia can reach swimming speeds of up to several mm/s with a highly alternating direction of motion. This makes it difficult to track individual cells with a microscope in free space, as the cell moves rapidly across the field of view and also out of focus. Several tracking methods exist to overcome this task. Hasegawa *et al.* presented a method of tracking the locomotion of an isolated micro-organism in a limited space.[4] Also more advanced techniques exist, where single cells can be followed with a motorized stage in 2D[5] and 3D.[6] Another approach is to use a multi-target tracking system as presented by Huang *et al.*[7] With a tracking

system, it is possible to follow the swimming path of a single cell, but measurements that require the cell to be held still in one place cannot be made with it. There are already a few methods described in the literature to hold individual cells in space. First, there are techniques that lead to temporary or complete immobilization of the cells by adding biochemical substances. The addition of ethanol (5% v/v) leads to a complete loss of cilia and thus complete immobilization.[8] This will, however, massively disrupt the physiology of the cells. Another method is to immobilize the cells to a substrate using, for example, the biochemical substance Cell-Tak™.[9] This method is less harmful to the cells but is also not reversible. Using electric or magnetic fields is another approach to establish contactless manipulation and trapping of cells.[10–12] There also exist microfluidic approaches. Lutz *et al.* described a new method that uses a gentle secondary flow to catch and release single cells, including motile cells, at predictable locations in 3D.[3] Another method uses filters with holes smaller than the specimen to mechanically entrain the cells to the bottom by negative pressure.[13] Acoustomicrofluidics can also be used to manipulate micro-organisms. Afzal *et al.* proposed a two-step acoustomicrofluidic separation method to isolate tardigrades from raw samples.[14] Läubli *et al.* combined an acoustically driven manipulation device with a micro-force sensor to freely rotate biological samples and quantify mechanical properties at multiple regions of interest within a specimen.[15] Therefore, the specimen had to be sedated before the procedure.

However, only a few of the methods presented are capable of reversibly trapping individual cells. And, none of them alone is able to track the swimming path of the same cell controllable and repeatedly. Therefore, we investigated different trapping mechanisms, to be able to compare the results of the different approaches and to exclude their influences on the measurement. Our first approach was to use standing surface acoustic waves (SSAW), similar to the technique used by Saito *et al.*, where they used ultrasonic standing waves.[16] As shown in our group before, SSAW are suitable to manipulate and arrange adherent cells.[17] Trapping cells with standing surface acoustic waves offers the possibility of confining cell movement to one dimension and slowing it down considerably.[18] A limitation here is the radio frequency (RF) power that can be applied, as it generates heat that could lead to cell death. In our second approach, we use a collagen fiber matrix to immobilize the cells. Here, the movement of the cells is limited to rotation. This method can be used for long-term measurements on a single cell, e.g., under variation of the culture medium. However, it is not reversible. The use of a microfluidic device allows us to reversibly trap single cells in small compartments and to monitor and analyze the swimming behavior over several minutes. Before and after reversible entrapment, the swimming speed is comparable, suggesting that entrapment does not have a large effect on cell behavior. Finally, we demonstrate the feasibility of membrane order measurements on living cells using the fluorescent dye 6-lauryl-2-dimethylaminonaphthalene (Laurdan).

MATERIALS AND METHODS

Culturing and solutions of *Paramecium caudatum*

Paramecium caudatum cells were grown in hay infusion media containing rice grains at 23 °C. Approximately half of the medium was replaced every four weeks. Prior to the experiments, paramecia were centrifuged at 800 g for 2 min. The cell pellet was then transferred to a buffer solution containing 1 mM $CaCl_2$, 1 mM KCl, 0.1 mM $MgSO_4$, and 1.5 mM MOPS (Sigma-Aldrich, St. Louis, MO, USA).

Trapping with standing acoustic waves

A pair of interdigital transducers (IDTs), oriented at an angle of 45° to the main propagation direction (X-direction) of the $LiNbO_3$ crystal, generates surface acoustic waves (SAW) with a wavelength of $\lambda_{SAW} = 100\,\mu$m at a sound path width $W = 1$ mm. The resonant frequency of each IDT is $f_{res} = 34.7$ MHz and the distance between the IDT is $l = 1.5$ mm. The RF signal is generated and divided by the frequency generator SML01 with an amplifier (gain factor G = 30 dB, AMP590033H-T) and a power splitter (ZFSC-2-4+). A glass slide (dimensions: 10×10 mm^2) is placed on two strips of adhesive tape, forming a channel with a height of approximately $h = 50\,\mu$m. This suppresses SAW-induced acoustic streaming due to vertical reflections at the top of the channel. In the regime dominated by the acoustic radiation force, microparticles are collected in the nodes of the partial standing sound-wave arising from reflection of microchannel walls.[19] Acoustic streaming on the other hand can be used for mixing at small Reynolds numbers.[20] However, this is an unintended effect here. The paramecium suspension is pipetted onto the SAW chip and drawn into the active area by capillary forces.

Collagen trapping

Paramecia were seeded in a chamber of an 8-well microslide (80 826, ibidi, Martinsried, Germany) in a collagen I solution on ice, which was then polymerized at room temperature in a culture chamber. For the working solution, the stock solution of collagen I (354249, Collagen I, High Concentration, Rat Tail, 100 mg—Corning Incorporated, NY, USA) is mixed with the cell suspension (V = 45% of total volume) and neutralized with sodium hydroxide (1M NaOH). By adding DPBS [Dulbecco's phosphate-buffered saline, DPBS (1×), ThermoFisher Scientific Inc., Waltham, MA, USA], a final collagen concentration of 1.85 mg/ml is achieved. For collagen fiber visualization, 0.5% (w/w) of collagen is replaced with fluorescein isothiocyanate (FITC)-conjugated type I collagen (AS-85111, AnaSpec, Seraing, Belgium). All components in contact with the collagen mixture were cooled in advance to prevent premature polymerization. The viability of the paramecium was checked by adding 1 μg of the fluorescent dye calcein green acetoxymethyl (AM) (56496-20X50UG, SA), which results in a final concentration of 1 μg/ml. The viability of the cells is observed by using the MDF-FITC-Filter (Thorlabs Inc., Newton, NJ, USA) (λ_{ex}:475/35; λ_{em}:530/43).

Microfluidic trapping

The elastomeric microchannels consist of a single layer of polydimethylsiloxane (PDMS) (Sylgard 184 Silicone Elastomer Kit, Dow Corning, Midland, MI, USA) (mixing ratio 10:1) and were fabricated by standard soft lithography. The PDMS block was permanently bonded to a glass slide using a plasma etching technique.

Three different channel designs were used in the experiments. Fluid flow was generated using either a syringe pump (PHD ULTRA, Harvard Apparatus, Holliston, MA, USA) or altitude reservoirs. Eppendorf tubes (1.5 ml, Eppendorf, Hamburg, Germany) were used as height reservoirs. For this purpose, a hole was punched in the lid through which a microfluidic tubing can be inserted. The Eppendorf tubes can be inserted into holders attached to the microscope for constant flow, where one holder is above and the other below the channel. For rapid pressure changes, the height difference can be varied manually by moving the Eppendorf tubes up or down. The maximum height difference is determined by the length of the microfluidic tubings. In the experiments, this was approx. 30 cm per tube. An inverted light microscope (Zeiss Axiovert 200, Carl Zeiss AG, Oberkochen, Germany) was used to observe the swimming behavior and trapping processes. The videos were recorded with a CCD camera (ORCA-05G, Hamamatsu, Hamamatsu, Japan) or a high-speed camera (FASTCAM Mini UX50, Photron, Ottobrunn, Germany).

Cell tracking

Videos of paramecia swimming behavior were analyzed using the public domain software package ImageJ (2.1.0, National Institutes of Health, Bethesda, MD, USA).[21] Using a macro-script, we can determine the position of cells on each image full automatically. Further analysis of the data is performed using Python (Python 3.8.3, Python Software Foundation).

Fluorescence measurements

The process for the optical measurements was adapted from Toyoda *et al.*[22] Paramecia were stained in a solution of 15 μM Laurdan for 30 min. The stock solution contained 2 mM Laurdan in dimethylformamide. The fluorescence of Laurdan was measured with an image splitting component (Hamamatsu, W-VIEW GEMINI, A12801-019). The selected filters were (438 ± 24) nm and (510 ± 42) nm, the beam splitter had a cut-off wavelength of 442 nm. Both images were simultaneously recorded on the chip of one single camera (ORCA-Flash 4.0 V3) with an exposure time of 80 ms. With the help of a computer, the GP of each pixel was calculated using $GP = (I_{438} - I_{510})/(I_{438} + I_{510})$ and plotted color-coded. Since the signal of the paramecium is significantly higher than the background, it could be easily extracted.

Temperature control of the microfluidic channels

To make temperature dependent measurements with the microfluidic channels, a small temperature sensor (dimensions: 2.3 × 2.1 × 0.9 mm, Nexensos M222 PT100, Heraeus, Hanau, Germany) was placed in the PDMS next to the experimental volume. The entire channel was heated or cooled by an external Peltier element with a recess in the middle to enable the microscopic measurements. The Peltier element was regulated by a TEC-Controller (Meerstetter Engineering, TEC-1091) via the computer.

RESULTS AND DISCUSSION

We here present three mechanisms for reversible and irreversible trapping of the micro-organism *Paramecium caudatum*. Our focus is on the microfluidic trapping, that can be used, e.g., for optical measurements to correlate cellular functions with the phase state. Figure 1(a) illustrates the acoustic trapping mechanism. By applying a standing acoustic wave field, the micro-organisms can be trapped in the pressure nodes. Figure 1(b) shows trapping in a collagen fiber matrix. Micro-organisms are incubated at low temperatures with an unpolymerized collagen mixture. After increasing the temperature, the micro-organisms are irreversibly trapped in the polymerized collagen matrix. Figure 1(c) demonstrates the microfluidic trapping. By applying a short pressure gradient, micro-organisms can be trapped and released in small compartments of a microfluidic channel. The high deformability allows the micro-organisms to pass these compartments unaffected. The trapping mechanisms and the resulting benefits are described in more detail below.

Trapping with standing surface acoustic waves

Figure 2(a) (Multimedia view) shows a microscope image of *Paramecium caudatum* trapped in a standing acoustic wave field. When the RF signal ($P_{IN} = 24$ dBm) is turned on, two surface acoustic waves with $P_{left/right} = 21$ dBm are generated from the left and right sides. The superposition of these two waves results in a standing wave. The free-floating cells are forced into the pressure nodes. The choice of the wavelength satisfies the one cell per acoustic well (OCPW) condition found by Collins *et al.*[23] with $\lambda_{SAW}/D_{Paramecium} \approx 3.3$, where $\lambda_{SAW} = 100\,\mu$m is the wavelength and $D_{Paramecium} \approx 30\,\mu$m is the average width of the cell. After a short resting time at a position, the cells move along the nodal lines (red trajectories) and thus follow the valleys in the potential landscape of the standing wave field. Figure 2(b) shows the velocity distribution of the micro-organisms when the RF signal is turned on. Clearly, compared to the undisturbed paramecium, there is a strong impairment of mobility. In most cases, the protozoan stays at one position but still occasionally reaches a velocity of up to $v = 0.6$ mm/s. RF powers of $P_{IN} = 27$ dBm or higher lead to rapid death of the cells due to heating of the medium. Active cooling mechanisms, e.g., using a Peltier element could allow for the application of higher power levels. Since the forces are not completely sufficient to compensate for the net movement of the cells even at high RF powers, long-term positioning by SAW is therefore not possible. Thus, a reduction of the degrees of freedom over a short period of time can be achieved with this method, but it is not sufficient for complete immobilization and we decided not to follow the SAW-approach here. Furthermore, applying a two-dimensionally patterned potential landscape by using two perpendicular delay lines brought no trapping-improvement as the cell length spans several nodes. Using 2D acoustic traps would need a second, delay line with a wavelength of about 500 μm oriented perpendicular to the first one. We did not implement this approach in our study.

Trapping in a collagen matrix

The use of polymerizing structural proteins such as collagen can also significantly limit the freedom of movement of paramecia.

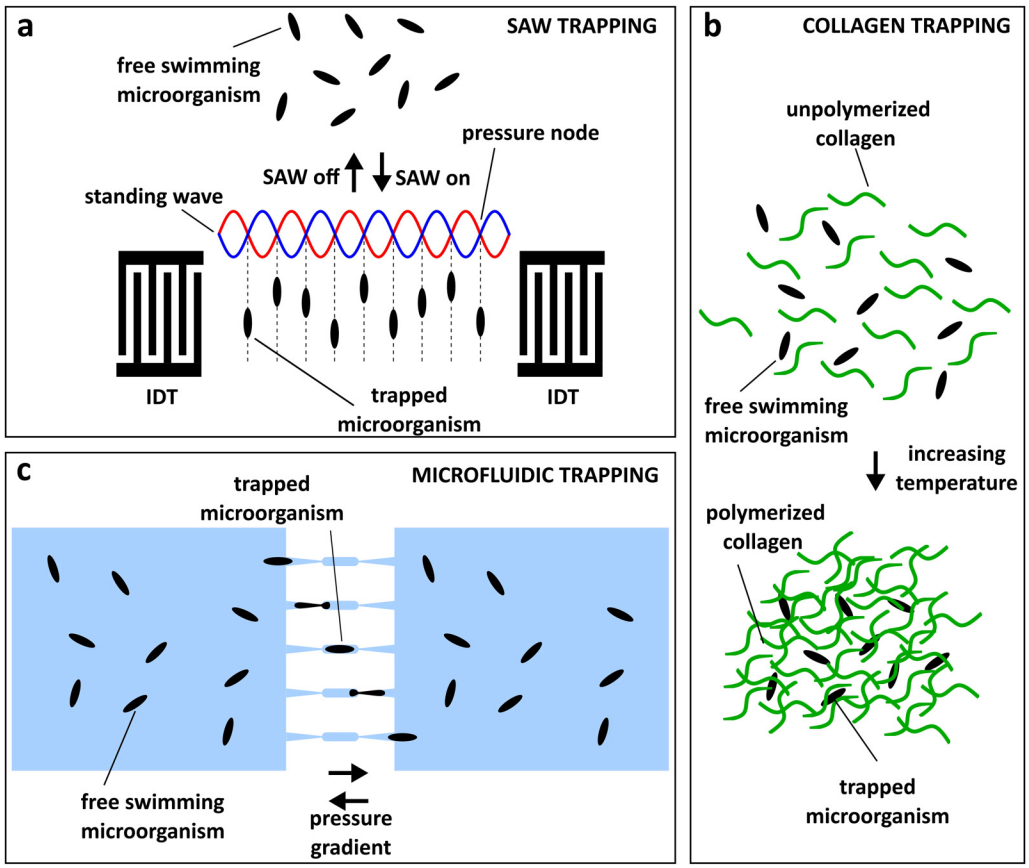

FIG. 1. Illustration of different trapping mechanisms for the micro-organism Paramecium caudatum. (a) By applying a standing acoustic wave field, the micro-organisms can be trapped in the pressure nodes. (b) Micro-organisms are incubated at low temperatures with an unpolymerized collagen mixture. After increasing the temperature, the micro-organisms are irreversibly trapped in the polymerized collagen matrix. (c) By applying a short pressure gradient, micro-organisms can be trapped and released in small compartments of a microfluidic channel. The high deformability allows the micro-organisms to pass these compartments unaffected.

Similar to the positioning of cells in an acoustic trap shown above, we can gently immobilize the agile cells using this method. To do this, we seed the paramecia in a collagen I solution and allow it to polymerize at room temperature in a cultivation chamber. Figure 3(a) shows a fluorescence image of a paramecium in polymerized collagen I in a chamber of an 8-well micro-slide. Here, the viability of the paramecium was checked by adding the fluorescent dye calcein green acetoxymethyl. The cell-permeable, non-fluorescent calcein derivative becomes fluorescent upon hydrolysis in the cytosol of a cell and thus serves as an indicator of active cell metabolism. The intense fluorescence signal of the paramecium consequently indicates a high viability of the cell. The structures around the paramecium represent the polymerized collagen fibers. The freedom of movement of the paramecium is restricted to such an extent that only rotation around its own axis is possible. This rotational motion can be seen in the individual images in Fig. 3(b). To illustrate the restricted freedom of movement, the rotation of the stationary paramecium is marked by a fixed point on the cell membrane. Thus, the effective swimming speed of the paramecium in collagen I is $v = 0$ mm/s, which corresponds to complete immobilization of the unicellular organism. Entrapping cells in a collagen fiber matrix restricts cell movement to rotation, allowing long-term measurements on a single cell, e.g., under variation of the culture medium. However, this trapping method is not reversible.

Microfluidic trapping

Our third method for trapping paramecia is based on a microfluidic approach. Inspired by existing microfluidic traps for lipid vesicles and cells,[24] we have developed a device that allows us to reversibly trap paramecia in small compartments, e.g., for fluorescence analysis, and to observe cell functions, e.g., swimming behavior. Figure 4 shows an overview of the different developmental stages of the setup. We started with a design with a series of traps and a free space where the swimming behavior of the micro-organism can be recorded [Fig. 4(a)]. The trap itself has a diameter of 10 μm at the smallest part. By applying a pressure gradient, the cells are forced into the traps. After releasing the pressure, the cells

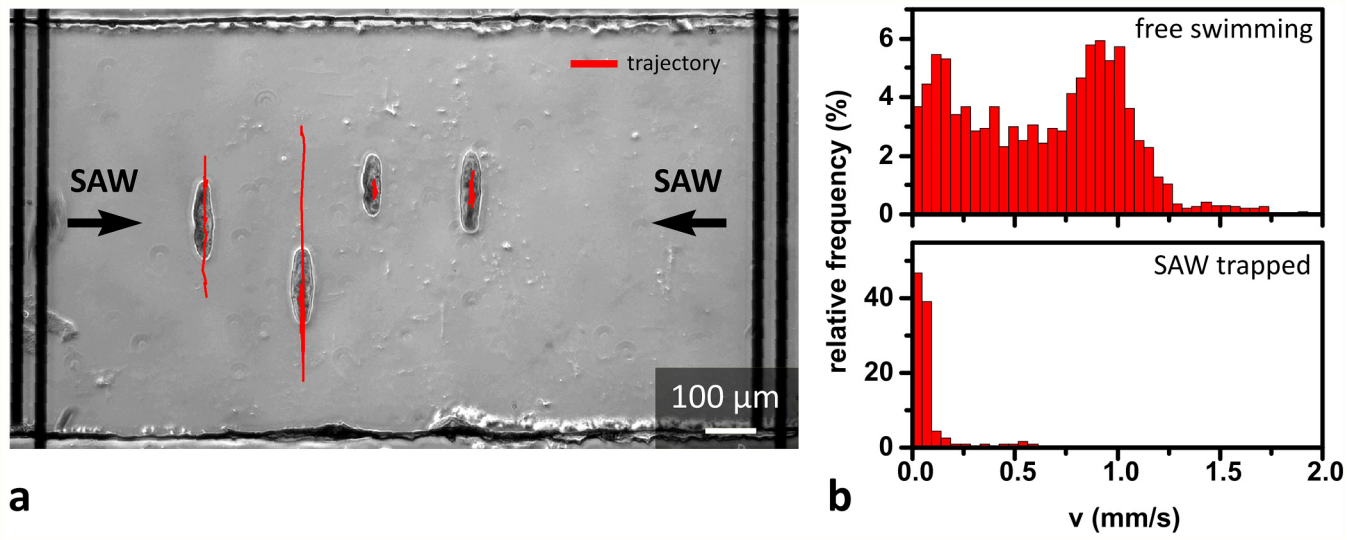

FIG. 2. Acoustic trapping of micro-organisms Paramecium caudatum. (a) Application of a standing acoustic wave field forces the micro-organisms into the pressure nodes. However, they are still able to move along a line of nodes as shown by the red trajectories. (b) The velocity distribution of the micro-organisms with SAW turned on. Compared to free swimming cells in a microfluidic channel with comparable height, the velocity is strongly reduced. Multimedia view: https://doi.org/10.1063/5.0084084.1

can leave the traps again. However, the cells get trapped here only in rare cases. Most of the paramecia can bypass the traps. Figure 4(b) shows the second version of the device, where there is no free space between the traps. This prevents the cells from bypassing a trap. In addition, the swimming area is provided with a barrier so that the cells cannot easily escape from the field of view. Figure 4(c) shows the final design of the trap device. The trap now has a barrier on both sides and is symmetrical. When a short pressure gradient is applied, the cells are forced into the trap and can also be released. A major advantage is that the cells cannot escape from the trap by themselves easily when the pressure is reduced. In addition, the device can be used from both sides.

We used two methods to create the pressure gradient. One is with a syringe pump and the other is with altitude reservoirs

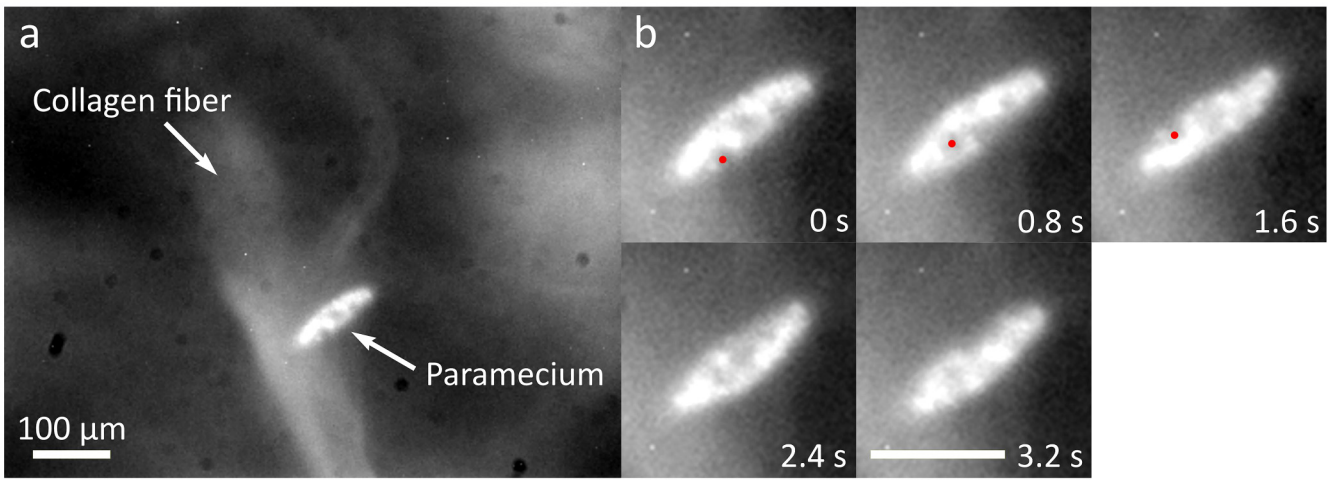

FIG. 3. Trapping of a micro-organism through a collagen matrix. (a) Fluorescence image (FITC) of a vital Paramecium caudatum in a polymerized fiber matrix, consisting of collagen I. (b) Orientation of the paramecium at specific time points. The strongly reduced freedom of movement leads to the rotation of the unicellular organism around its own axis. The rotational motion is marked by a red dot. Scale bars = 100 μm.

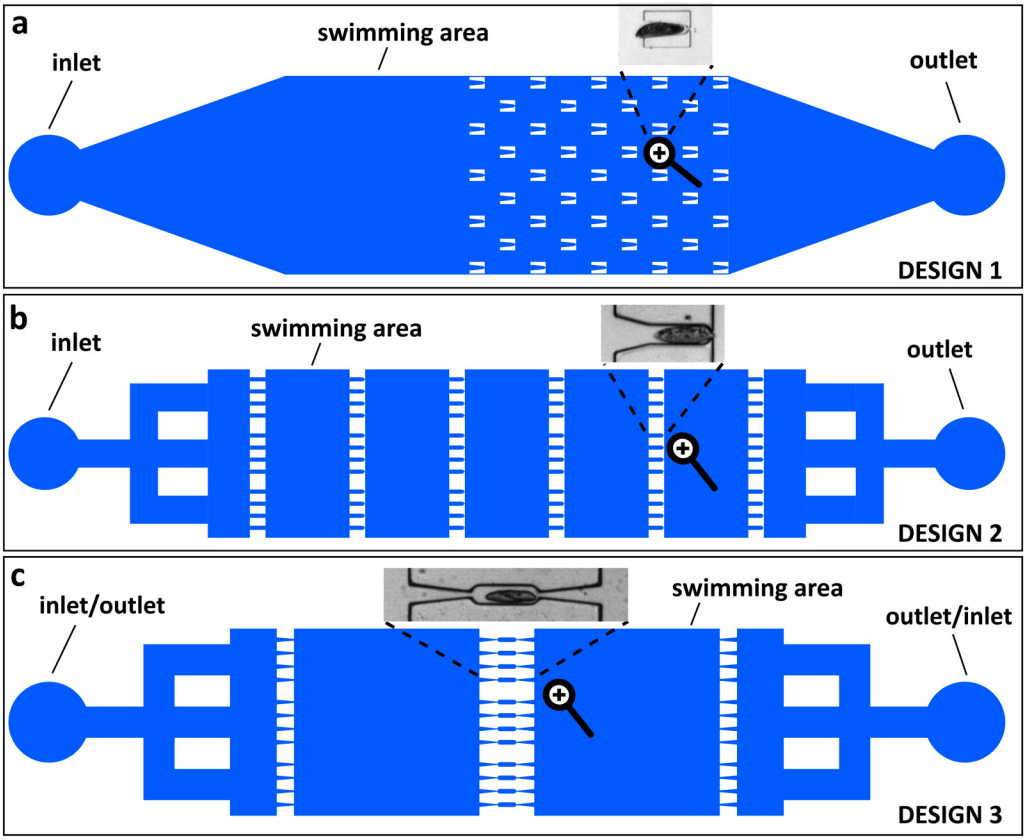

FIG. 4. Development of a microfluidic trapping device for the mobile micro-organism Paramecium caudatum. (a) First design with an array of traps and free space in which the swimming behavior of the micro-organism can be tracked. By applying a pressure gradient, the cells are forced into the traps. (b) Second design of the device, where there is no free space between the traps. This prevents the cells from bypassing a trap, resulting in a higher trapping efficiency. (c) Final design of the trapping device. The trap has a barrier on both sides and is symmetrical. When a short pressure gradient is applied, the cells are forced into the trap and can also be released. A major advantage is that the cells cannot escape from the trap by themselves when the pressure gradient is reduced.

(max pressure of about 5 kPa). With the syringe pump, a flow rate of about 1 ml/h is applied. Once the cell enters a trap, the flow is stopped to prevent the cell from being pushed through the trap. However, very rapid changes are experimentally challenging. With the altitude reservoir, there are several advantages. First, pressure changes can be achieved continuously and very quickly by simply changing the altitude. Also, it is possible to apply both negative and positive pressure gradients in both directions. This allows simultaneous pushing and pulling on the cells using a lower reservoir connected to the outlet, and a higher reservoir connected to the inlet. According to Tsai *et al.*,[25] this can influence the deformation of the cells.

Figure 5(a) (Multimedia view) shows an overlay of different time steps of micrographs during an attempt to trap paramecia in a design 1 microfluidic channel. When a pressure gradient is applied, most cells pass through the traps as they are not oriented parallel to the direction of flow when approaching a trap. In the following, the cells meander through the traps in most cases as shown. Only in rare cases a cell actually got stuck in a trap. Figures 5(b) (Multimedia view) and 5(c) (Multimedia view) show the trapping process for the other two designs. When a pressure gradient is applied, the cells are deflected from their original swimming path and forced into a trap. Before the pressure gradient is applied, the cell swims sideways. After the pressure gradient is applied, the cells are accelerated downward toward the traps. This can be seen especially in Fig. 5(c) by the motion blur caused by the higher velocity.

A major difference between the trap shown in Fig. 5(b) (design 2) and the one in Fig. 5(c) (design 3) is that the trap in design 2 is not constricted on both sides. In this case, the pressure gradient must be kept constant to keep the cells in the trap. In the other case (design 3), the cells remain trapped even when the pressure is reduced, because the trap is constricted from both sides. This behavior is demonstrated in Figs. 5(d) and 5(e) by tracking the swimming velocity during a trapping event for both designs. At the beginning, without a pressure gradient, the cells can freely swim in the channel. When a pressure gradient is applied, the cells are forced into the traps and the velocity drops to zero (red area). After the pressure is released, the cell can escape from the trap in design 2, as can be seen by the velocity, which is no longer zero.

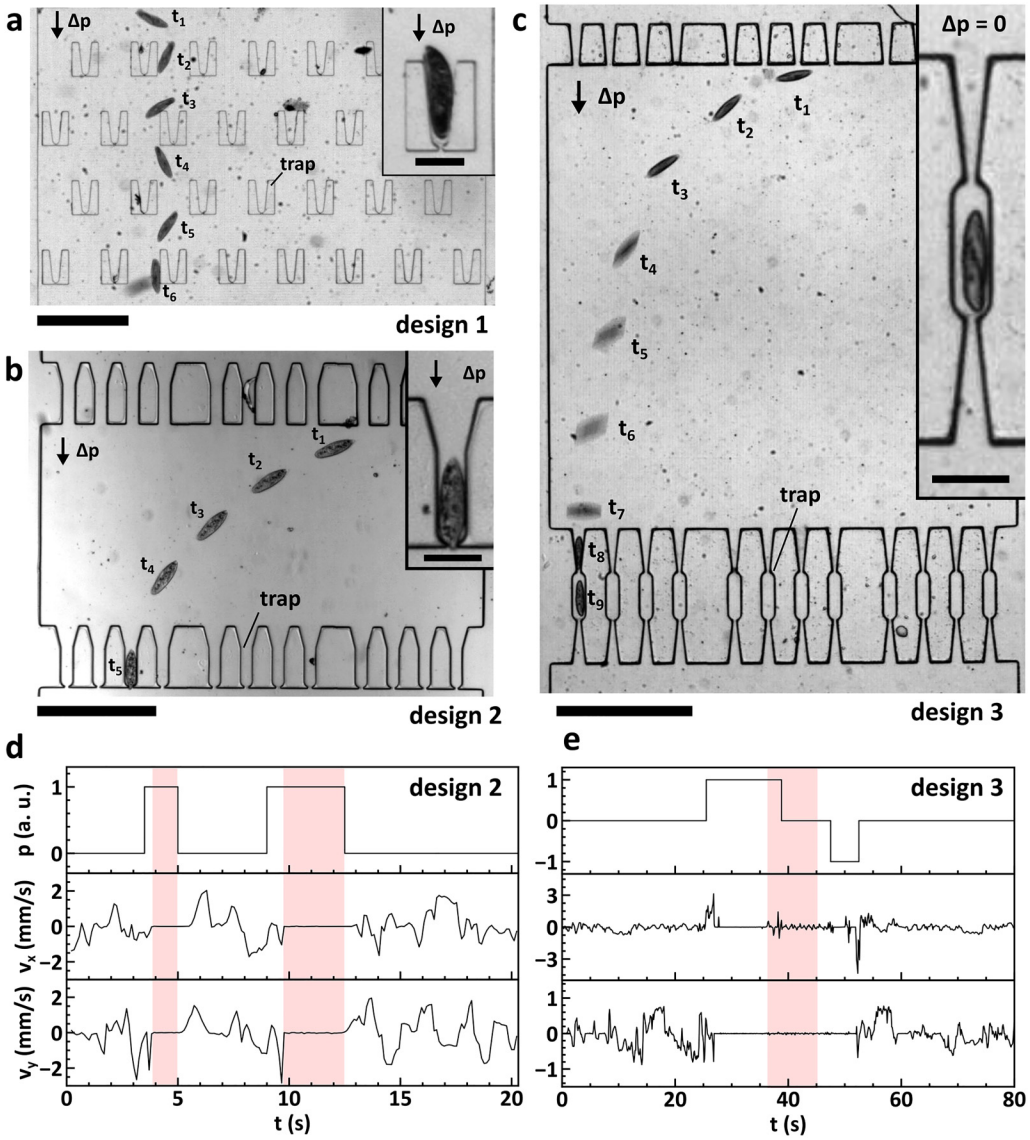

FIG. 5. Different microfluidic trapping designs for the micro-organism Paramecium caudatum and observation of the swimming velocity. (a) Most cells can pass through the traps. Only in rare cases, a cell gets stuck in a trap. (b) and (c) when a pressure gradient is applied, cells are deflected from their original swimming path and forced into a trap. Scale bars = 500 μm and 100 μm (insets). (d) Without a pressure gradient, the cells can swim freely in the channel. When a pressure gradient is applied, the cells are forced into the traps and the velocity drops to zero (red area). With the trap constricted on only one side, the pressure gradient must be kept constant to keep the cells in the trap. (e) With the trap constricted on both sides, the cells remain trapped even when the pressure drops. Multimedia views: https://doi.org/10.1063/5.0084084.2; https://doi.org/10.1063/5.0084084.3; https://doi.org/10.1063/5.0084084.4

By applying a second pressure gradient, the cell can be trapped again. In design 3, the velocity remains zero even though there is no longer a pressure gradient applied. Consequently, the cell is still in the trap. Only after applying a negative pressure gradient the cell can be released from the trap again.

Figure 6(a) (Multimedia view) shows a time series of the micro-organism *Paramecium caudatum* passing through a microfluidic trap of design 2. When a continuous pressure drop is generated, the cell is pushed through a trap in some cases. Initially, only a small part of the cell membrane is pushed through the trap. As time progresses, more and more of the cell is pressed to the other side. After about 14 s, almost the entire cell is forced through the trap. In the following, the cell can then pass through the trap, which is not shown here. With the trap, which has a diameter of

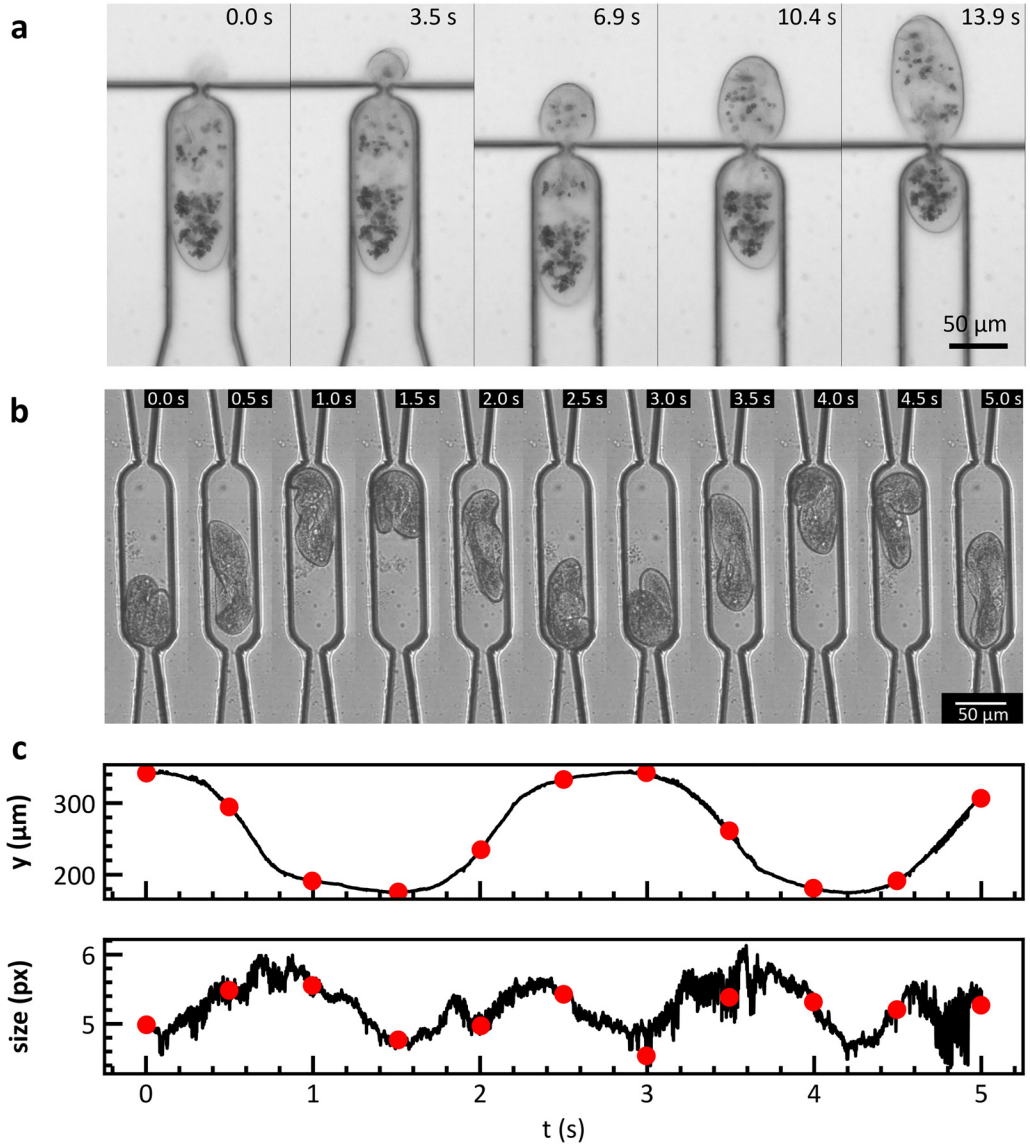

FIG. 6. Time series of the micro-organism Paramecium caudatum passing through a microfluidic trap of design 2 and caught in a microfluidic trap of design 3. (a) When a continuous pressure gradient is applied, the cell is pushed through a trap of design 2 that has a diameter of 5 μm at its smallest point. The cell, which has a diameter of 50 μm at its largest point, can be compressed by a factor of 10 without optical detectable damage. This process impressively demonstrates the extremely high deformability of the cell. (b) Time series of the cell moving in a microfluidic trap of design 3. The cell can float up and down in the trap, even if the dimensions of the channel are only slightly higher than the cell itself. (c) Tracked position and size of the cell in the trap. The cell is largest when it is in the center of the trap and smallest in the corner of the trap where the cell is bent. Multimedia views: https://doi.org/10.1063/5.0084084.5; https://doi.org/10.1063/5.0084084.6

5 μm at its smallest point, the cell, which has a diameter of 50 μm at its largest point, can be compressed by a factor of 10 without causing any optically detectable damage. This process impressively demonstrates the extremely high deformability of the cell. However, this makes it difficult to keep the cells in the trap for an extended period of time, which is another reason why design 3 is advantageous. Figure 6(b) (Multimedia view) shows a time series of the micro-organism *Paramecium caudatum* caught in a microfluidic trap. The cell can float up and down in the trap, even if the dimensions of the channel are only slightly wider and higher than the cell itself. Due to its extremely high deformability, the cell is able to bend at the corners and thus change direction. Right in the corner the cell is completely folded. In the middle of the trap the cell is stretched again. This is another example that demonstrates the

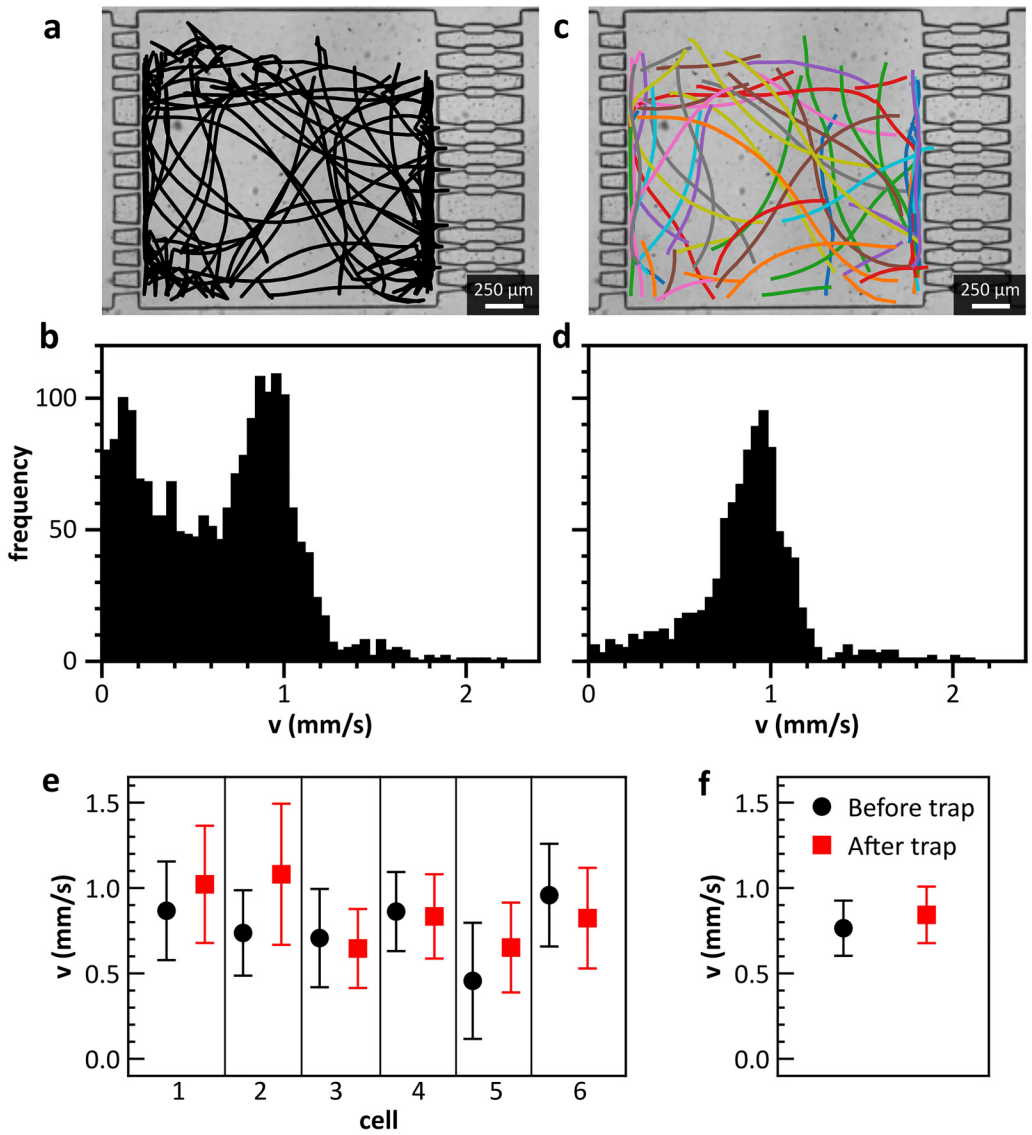

FIG. 7. Tracking the swimming behavior of a single micro-organism in a microfluidic chamber with a height of 50 μm and comparison of swimming behavior before and after trapping. (a) The swimming path of a single micro-organism tracked by an object recognition algorithm. (b) The calculated velocity distribution of the moving cell shows two peaks. The lower peak can be attributed to the direction change events. (c) To filter out the lower peak, we introduced the condition that every time the change in velocity angle is greater than 45°, a new trace starts. In addition, we only count traces with a length greater than 200 μm. (d) The calculated velocity distribution of the filtered tracks is now about normally distributed and shows its maximum near 1 mm/s. (e) Mean swimming speed of individual cells observed over a few minutes before (black) and after (red) the trapping event. Error bars show the standard deviation. (f) Mean velocity of all cells before and after trapping. Error bars show the standard deviation (n = 6). No change in swimming speed can be seen within the error range. Multimedia view: https://doi.org/10.1063/5.0084084.7

extremely high deformability of the cell. Figure 6(c) shows the position in the trap and the corresponding size of the cell. In the center of the trap, the paramecia is stretched, resulting in a large size. In the corner, it is folded, resulting in the smallest size. Thus, the traced size is a measure of how much the cell is bent.

In the next step, we observed the swimming behavior of a single micro-organism in our microfluidic device. Figure 7(a) (Multimedia view) shows the swimming path of a single micro-organism tracked by an object recognition algorithm. Due to the limited area, many events occur where the cell must change its direction. Figure 7(b) shows the calculated velocity distribution of the moving cell with two peaks. The lower peak can be attributed to the direction change events. The higher peak is attributed to straight swimming. As we are interested in the straight

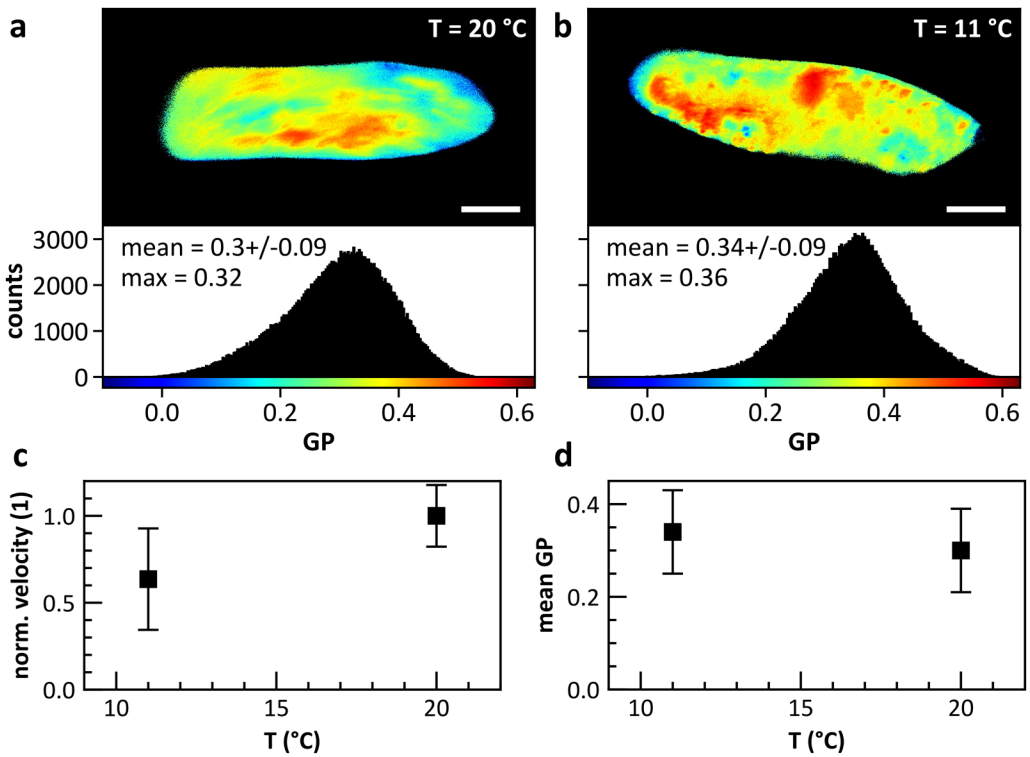

FIG. 8. Optical measurement of membrane fluidity of trapped paramecium and comparison of temperature dependent swimming velocity and GP value. (a) Pixel-wise color-coded GP of a paramecium stained with Laurdan at 20 °C. (b) GP of the same paramecium at 11 °C. At lower temperatures, the distribution of GP values shifts to higher values. (c) Normalized swimming velocity in dependency of the temperature. The error bars indicate the standard deviation of the different calculated swimming velocities at the same temperature with the same organism. (d) GP value in dependency of the temperature. The swimming velocity decreases with decreasing temperature and therefore with decreasing membrane fluidity.

swimming, we introduced a filter scheme. Figure 7(c) shows the filtered traces. We introduced the condition that every time the change in velocity angle is greater than 45°, a new trace starts. In addition, we only count traces with a length greater than 200 μm. Thus, the complete tracking path is split into several traces. The calculated velocity distribution of the filtered tracks is now about normally distributed and shows its maximum near 1 mm/s [Fig. 7(d)]. A crucial requirement for our microfluidic device is minimal influence of the entrapment on the behavior of the micro-organism. Therefore, we observed the swimming behavior before and after trapping. Figure 7(e) shows the mean swimming speed of individual cells observed over a period of at least 3 min before (black) and after (red) trapping. The error bars show the standard deviation. In some cases, the velocity is higher after capture, while in others, it is lower. There is no clear trend that swimming speed changes drastically after capture. Figure 7(f) shows the mean velocity of all cells before and after trapping. The error bars also show the standard deviation. No change in swimming speed can be seen within the error range, indicating that trapping does not have a large effect on the behavior of the cells.

Optical measurements

To measure membrane fluidity, the fluorescence dye Laurdan can be used. The sensitivity of Laurdan excitation and emission spectra to the physical state of the membrane arises from dipolar relaxation processes in the membrane region surrounding the Laurdan molecule.[26] However, to apply such measurements to single cells with a good lateral resolution, they have to be immobilized. When previously stained paramecia were trapped in our microfluidic channel of design 3, the fluorescent signal of Laurdan could be easily measured. Figure 8(a) shows the pixel-wise color-coded GP (see Materials and Methods section for details) of a paramecium measured at 20 °C. In the lower half, the distribution of all measured GP values is shown, together with the mean and the maximum of this distribution. Figure 8(b) shows the same paramecium measured at 11 °C. At lower temperatures, the distribution of GP values shifts to higher values which fits the results of Toyoda *et al.*[22]

One advantage of the microfluidic channels is the possibility to release the specimen between the measurements to analyze their swimming behavior. Figures 8(c) and 8(d) show the measured swimming velocities at 11 and 20 °C compared to the mean GP

from Figs. 8(a) and 8(b). The mean GP value increases with decreasing temperature, which means that the spectrum of Laurdan shifts to smaller wavelengths. The swimming velocity decreases with decreasing temperature and therefore with decreasing membrane fluidity. Swimming speed is normalized here for better comparison between different paramecia. This correlation should be investigated in further measurements.

CONCLUSION

We demonstrated three different methods of irreversible and reversible trapping of motile protozoa *Paramecium caudatum*. We found that SAW trapping restricts cell movement to one dimension. However, this method leads to rapid cell death at high RF power. Trapping with collagen I is gentler toward the cells and opens the possibility for long-term measurements. Here, the movement of the cells is limited to rotation along the major axis. The disadvantage is that the method is not reversible. In contrast, our microfluidic approach allows reversible trapping of the cells. Due to their extremely high deformability, the cells can be pushed into small compartments without visually detectable damage. Moreover, the technique allows not only the trapping of cells, but also the tracking of their swimming behavior. We could not detect a negative influence of the trapping process on the swimming behavior of the cells. Consequently, the technique is suitable, e.g., for the correlation of optical measurements of the membrane order, where the cell has to be held relatively stationary, and tracking of a cellular function, like the swimming behavior.

ACKNOWLEDGMENTS

The authors would like to acknowledge funding by Nanosystems Initiative Munich (NIM), the Center for NanoScience (CeNS), and the Augsburg Centre for Innovative Technologies (ACIT).

Conflict of Interest

The authors have no conflicts to disclose.

Author Contributions

L.G.S., M.F.S., and C.W. are involved in conceptualization; L.G.S., A.P., and M.S.B. in methodology; L.G.S., A.P., and M.S.B. in investigation; M.F.S. and C.W. in resources; and L.G.S. and C.W. in writing the original draft. All authors were involved in writing, reviewing, and editing. M.F.S. and C.W. were involved in supervision and funding acquisition. All authors have read and agreed to the published version of the manuscript.

DATA AVAILABILITY

The data that support the findings of this study are available from the corresponding author upon reasonable request.

REFERENCES

[1]R. Wichtermann, *The Biology of Paramecium* (Plenum Press, New York, 1986).
[2]M. E. Lidstrom and D. R. Meldrum, "Life-on-a-chip," Nat. Rev. Microbiol. **1**(2), 158–164 (2003).
[3]B. R. Lutz, J. Chen, and D. T. Schwartz, "Hydrodynamic tweezers: 1.: Noncontact trapping of single cells using steady streaming microeddies," Anal. Chem. **78**(15), 5429–5435 (2006).
[4]K. Hasegawa, A. Tanakadate, and H. Ishikawa, "A method for tracking the locomotion of an isolated microorganism in real time," Physiol. Behav. **42**(4), 397–400 (1988).
[5]X. Fei, Y. Igarashi, and K. Hashimoto, "2D tracking of single paramecium by using parallel level set method and visual servoing," in *2008 IEEE/ASME International Conference on Advanced Intelligent Mechatronics* (IEEE, 2008), pp. 752–757.
[6]K. Yamato, H. Chiba, and H. Oku, "High speed three dimensional tracking of swimming cell by synchronous modulation between TeCE camera and TAG lens," IEEE Robot. Autom. Lett. **5**(2), 1907–1914 (2020).
[7]K.-N. Huang, H.-H. Chen, and Y.-S. Yeh, "Development of a multi-target tracking system for paramecia," in *2011 4th International Conference on Biomedical Engineering and Informatics (BMEI)* (IEEE, 2011), Vol. 1, pp. 259–262.
[8]B. Y. H. Machemer and A. Ogura, "Ionic conductances of membranes in ciliated and deciliated paramecium," J. Physiol. **296**(1), 49–60 (1979).
[9]W. E. Bell, R. Hallworth, T. A. Wyatt, and J. H. Sisson, "Use of a novel cell adhesion method and digital measurement to show stimulus-dependent variation in somatic and oral ciliary beat frequency in paramecium," J. Eukaryotic Microbiol. **62**(1), 144–148 (2015).
[10]K. Guevorkian and J. M. Valles, Jr., "Aligning *Paramecium caudatum* with static magnetic fields," Biophys. J. **90**(8), 3004–3011 (2006).
[11]R. Venu, B. Lim, X. H. Hu, I. Jeong, T. S. Ramulu, and C. G. Kim, "On-chip manipulation and trapping of microorganisms using a patterned magnetic pathway," Microfluidics Nanofluidics **14**(1–2), 277–285 (2013).
[12]Z. Ye and M. Sitti, "Dynamic trapping and two-dimensional transport of swimming microorganisms using a rotating magnetic microrobot," Lab Chip **14**(13), 2177–2182 (2014).
[13]A. Kulkarni, I. Elices, N. Escoubet, L.-L. Pontani, A. M. Prevost, and R. Brette, "A simple device to immobilize protists for electrophysiology and microinjection," J. Exp. Biol. **223**(12), jeb219253 (2020).
[14]M. Afzal *et al.*, "Acoustomicrofluidic separation of tardigrades from raw cultures for sample preparation," Zool. J. Linn. Soc. **188**(3), 809–819 (2020).
[15]N. F. Läubli *et al.*, "3D mechanical characterization of single cells and small organisms using acoustic manipulation and force microscopy," Nat. Commun. **12**(1), 1–11 (2021).
[16]M. Saito, N. Kitamura, and M. Terauchi, "Microorganism manipulation and microparticle arrangement by the use of ultrasonic standing waves," BioMEMS Smart Nanostruct. **4590**, 26–37 (2001).
[17]M. S. Brugger, S. Grundeen, A. Doyle, L. Theogarajan, A. Wixforth, and C. Westerhausen, "Orchestrating cells on a chip: Employing surface acoustic waves towards the formation of neural networks," Phys. Rev. E **98**(1), 012411 (2018).
[18]M. S. Brugger, "Sensorik, aktorik und stimulation vitaler zellen unter verwendung akustischer oberflächenwellen," Ph.D. dissertation (Universiät Augsburg, 2021).
[19]M. Travagliati, R. J. Shilton, M. Pagliazzi, I. Tonazzini, F. Beltram, and M. Cecchini, "Acoustofluidics and whole-blood manipulation in surface acoustic wave counterflow devices," Anal. Chem. **86**(21), 10633–10638 (2014).
[20]K. Sritharan, C. J. Strobl, M. F. Schneider, A. Wixforth, and Z. Guttenberg, "Acoustic mixing at low Reynold's numbers," Appl. Phys. Lett. **88**(5), 054102 (2006).
[21]C. A. Schneider, W. S. Rasband, and K. W. Eliceiri, "NIH image to ImageJ : 25 years of image analysis," Nat. Methods **9**(7), 671–675 (2012).
[22]T. Toyoda, Y. Hiramatsu, T. Sasaki, and Y. Nakaoka, "Thermo-sensitive response based on the membrane fluidity adaptation in *Paramecium multimicronucleatum*," J. Exp. Biol. **212**(17), 2767–2772 (2009).
[23]D. J. Collins, B. Morahan, J. Garcia-bustos, C. Doerig, M. Plebanski, and A. Neild, "Two-dimensional single-cell patterning with one cell per well driven by surface acoustic waves," Nat. Commun. **6**(1), 1–11 (2015).

[24]D. Di Carlo, N. Aghdam, and L. P. Lee, "Single-cell enzyme concentrations, kinetics, and inhibition analysis using high-density hydrodynamic cell isolation arrays," Anal. Chem. **78**(14), 4925–4930 (2006).
[25]C. D. Tsai, S. Sakuma, F. Arai, and M. Kaneko, "What is the difference of cell deformation between push and pull?," in *18th International Conference on Miniaturized Systems for Chemistry and Life Sciences, MicroTAS 2014* (Chemical and Biological Microsystems Society, 2014), pp. 793–795.
[26]T. Parasassi, G. De Stasio, G. Ravagnan, R. M. Rusch, and E. Gratton, "Quantitation of lipid phases in phospholipid vesicles by the generalized polarization of Laurdan fluorescence," Biophys. J. **60**(1), 179–189 (1991).